

Thermal and electrical properties of $\text{Ba}_2\text{In}_2\text{O}_5$ substituted for In-site by rare earth elements

Tuan Q. Ta, Toshihide Tsuji*, Yasuhisa Yamamura

*School of Materials Science, Japan Advanced Institute of Science and Technology,
1-1 Asahidai, Nomi, Ishikawa 923-1292, Japan*

Available online 24 June 2005

Abstract

$\text{Ba}_2(\text{In}_{1-x}\text{R}_x)_2\text{O}_5$ ($x=0, 0.05, 0.1$; $\text{R}=\text{Sc, Lu, Yb, Y, Dy, Gd, Sm}$) were synthesized by a solid-state reaction method, and all the prepared samples were confirmed to be a single phase by XRD. The lattice volume increased with increasing ionic radius of the substituents, and the slope in the plot of the lattice volume against the ionic radius was changed around the ionic radius of Y^{3+} or Dy^{3+} . The order–disorder transition temperatures of oxygen vacancies of all the prepared samples were determined by electrical conductivity measurement. The transition temperatures of the samples substituted by larger (or smaller) ions in the ionic radius than In ion were larger (smaller) than that of un-substituted $\text{Ba}_2\text{In}_2\text{O}_5$, probably due to the preferred site of substituent to either octahedral InO_6 site or tetrahedral InO_4 site.

© 2005 Elsevier B.V. All rights reserved.

Keywords: Oxide ion conduction; Order–disorder transition; Rare earth element; $\text{Ba}_2\text{In}_2\text{O}_5$; Brownmillerite-type structure

1. Introduction

Oxide ion conductors have been studied for many applications to oxygen sensors, oxygen-permeable membrane reactors and solid oxide fuel cells. A lot of investigations have been conducted in order to find out a high oxide ion conductor or to elucidate the conduction mechanism of the oxide ion [1–4].

$\text{Ba}_2\text{In}_2\text{O}_5$, having the brownmillerite-type structure, is one of candidates for the high oxide ion conductor at high temperature. The stoichiometric $\text{Ba}_2\text{In}_2\text{O}_5$ is essentially super-structural form of the cubic perovskite, in which one-sixth of the oxygen atoms are replaced by an ordered array of vacancies along the [1 0 1] direction as shown in Fig. 1. $\text{Ba}_2\text{In}_2\text{O}_5$ showed an order–disorder transition of oxygen vacancies around transition temperature $T_t = 1200$ K and particularly, had a high oxygen ion conductivity above transition temperature T_t comparable to yttria-stabilized zirconia of the most widely used oxygen ion conductor [5,6]. These facts suggest that the shift of transition temperature T_t to a

lower temperature might result in high oxide ion conductivity at relatively low temperatures. So far, a lot of studies have been carried out in order to stabilize the high-temperature phase to lower temperature, but there are few researches emphasizing on the nature of the order–disorder transition. Firstly, Prasanna et al. [7] suggested from high-temperature step scanning calorimetry that the order–disorder transition involved only a small fraction of the oxygen vacancies and implied extensive short-range order in the high-temperature phase. Adler et al. [8] concluded from the combination of NMR and XRD techniques that the order–disorder transition at around 1200 K only involved oxygen atoms O(3) in the tetrahedral layer, which was between layers of octahedral coordinated In atoms, and the material retained an orthorhombic layered structure with a space group $Icmm$ until about 1350 K, where the material became a cubic structure. Using high-temperature XRD, the phase between 1200 and 1350 K was assigned to a tetragonal structure with a space group $I4cm$ by Speakman et al. [9]. The number of mobile oxygen ions in the structure increased continuously in the intermediate phase and implied that at 1200 K vacancies undergo a two-dimensional order–disorder transition. The effect of substitution for In site by the elements, such as Y, Yb, Sc and

* Corresponding author. Tel.: +81 761 51 1520; fax: +81 761 51 1149.
E-mail address: tsuji@jaist.ac.jp (T. Tsuji).

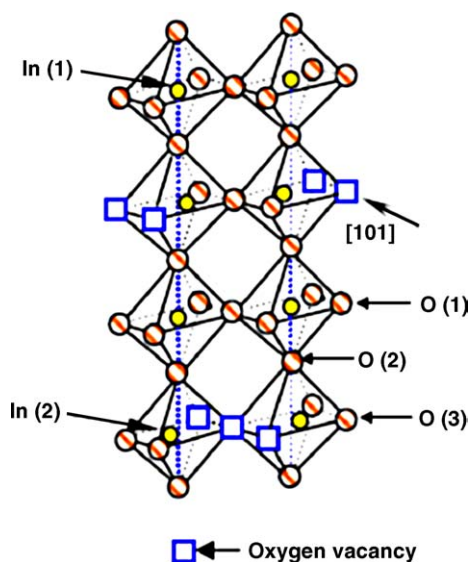


Fig. 1. Ideal brownmillerite structure of $\text{Ba}_2\text{In}_2\text{O}_5$ at room temperature.

Ga on the order–disorder transition was investigated from the viewpoint of the unit cell free volume [10], whereas those of both sites, such as Ga for In and Sr for Ba were inspected from the tolerance factor [11]. However, the effects of ionic radius of rare earth element and its content on the order–disorder transition of substituted $\text{Ba}_2\text{In}_2\text{O}_5$ still were ambiguously explained.

In this work, we investigate the effects of ionic radii and substituted content of rare earth elements into In site on thermal and electrical properties of substituted $\text{Ba}_2\text{In}_2\text{O}_5$ in order to understand precisely the mechanism of this order–disorder transition.

2. Experimental

All the samples of $\text{Ba}_2(\text{In}_{1-x}\text{R}_x)_2\text{O}_5$ ($x=0, 0.05, 0.1$) were prepared by a solid-state reaction method, using BaCO_3 , In_2O_3 and R_2O_3 ($\text{R}=\text{Sm}, \text{Gd}, \text{Dy}, \text{Yb}, \text{Lu}, \text{Sc}, \text{Y}$) as starting materials. The required quantities of starting materials were mixed in *n*-hexane for 1 h, and the mixed powders were calcined at 1273 K for 10 h in air. The obtained powders were reground in *n*-hexane for another 1 h and then pressed into pellets under a pressure of 20 MPa. The pellets were then sintered at 1573 K for 10 h in Ar gas atmosphere.

The samples prepared were characterized by X-ray powder diffractometer RINT 2500 V using $\text{Cu K}\alpha$ radiation at room temperature. Electrical conductivity measurement of the sintered samples of about 10 mm in diameter and about 2 mm in thickness was carried out in the temperature range from room temperature to 1323 K by a four-probe method. Thermal properties of the samples were measured in air by TG–DTA method at the heating rate of 10 K/min in the temperature range from room temperature to 1323 K.

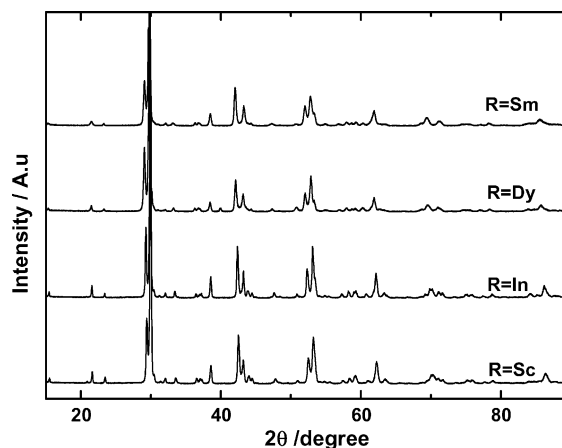


Fig. 2. Typical XRD patterns of $\text{Ba}_2(\text{In}_{0.9}\text{R}_{0.1})_2\text{O}_5$ ($\text{R}=\text{Sm}, \text{Dy}, \text{In}, \text{Sc}$) system.

3. Results and discussion

Typical XRD patterns of the prepared samples $\text{Ba}_2(\text{In}_{0.9}\text{R}_{0.1})_2\text{O}_5$ ($\text{R}=\text{Sm}, \text{Dy}, \text{In}, \text{Sc}$) are shown in Fig. 2. The results confirmed that all the samples were a single phase with an orthorhombic symmetry over the whole composition range, $0 \leq x \leq 0.1$. The lattice constants of the samples were determined using the XRD results by a least-squares calculation. The lattice constants of $\text{Ba}_2\text{In}_2\text{O}_5$ were calculated to be $a = 596.5$ pm, $b = 1671.6$ pm and $c = 609.3$ pm, which were in good agreement with the previous reports by Rietveld analysis [9,12,15]. The densities of all samples were calculated to be around 80% of theoretical value.

Fig. 3 shows the unit cell volume, V , of $\text{Ba}_2(\text{In}_{1-x}\text{R}_x)_2\text{O}_5$ ($x=0, 0.05, 0.1$) samples as a function of substituted x content. In the present study, a unit cell was selected according to the primitive lattice of the perovskite structure. A good linear relationship between V and x is seen in figure, indicating that all substituted rare earth ions form solid solution up to $x=0.1$ with the mother compound. The unit cell volume is

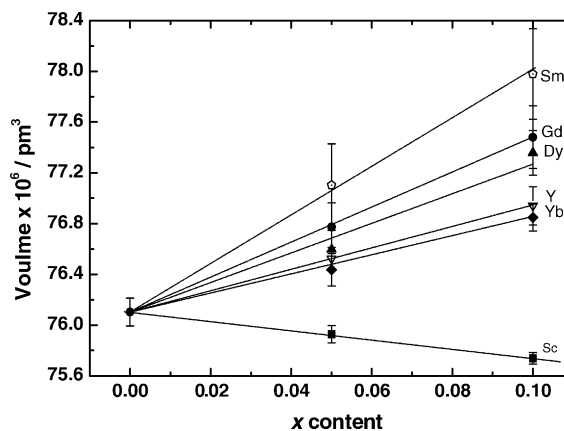


Fig. 3. Unit cell volume of $\text{Ba}_2(\text{In}_{1-x}\text{R}_x)_2\text{O}_5$ ($\text{R}=\text{Sc}, \text{Yb}, \text{Y}, \text{Dy}, \text{Gd}, \text{Sm}$) system as a function of x content.

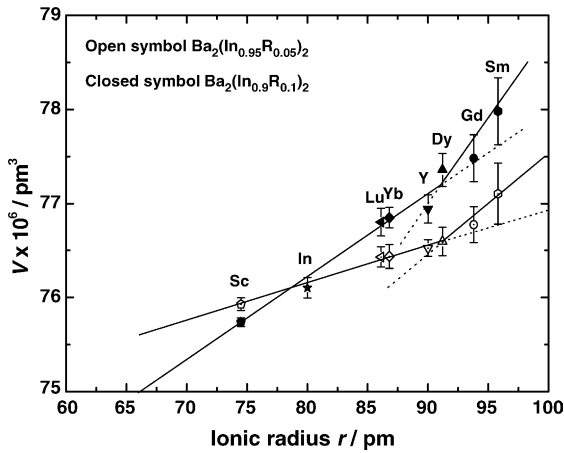


Fig. 4. Unit cell volume, V , of $\text{Ba}_2(\text{In}_{1-x}\text{R}_x)_2\text{O}_5$ system as a function of substituents' ionic radius.

plotted as a function of substituents' ionic radius in Fig. 4. The unit cell volume increases linearly with increasing the ionic radius of the substituted ions, but the slope changes around ionic radius of Y^{3+} or Dy^{3+} element. The change in the slope may be related to the formation of $\text{Ba}_2\text{R}_2\text{O}_5$. The Sc, Lu, Yb, Y and Dy elements form $\text{Ba}_2\text{R}_2\text{O}_5$ (Sc, Lu, Yb, Y, Dy) having a tetragonal structure, whereas the Sm and Gd elements do not form $\text{Ba}_2\text{R}_2\text{O}_5$.

Fig. 5 shows the typical Arrhenius plots of the electrical conductivity of $\text{Ba}_2(\text{In}_{1-x}\text{R}_x)_2\text{O}_5$ ($\text{R} = \text{Sc}, \text{In}, \text{Yb}, \text{Y}, \text{Sm}$) system. An abrupt increase in electrical conductivity of un-doped $\text{Ba}_2\text{In}_2\text{O}_5$ is seen in figure. The transition temperature, T_t , of $\text{Ba}_2(\text{In}_{1-x}\text{R}_x)_2\text{O}_5$ system due to oxygen vacancies was determined from two extrapolation lines of the electrical conductivity before and after phase transition as seen for a typical doped Sc ion in Fig. 5, and transition temperature of each substituted sample is also shown by the arrow in Fig. 5. The transition temperature of 1200 K for un-doped $\text{Ba}_2\text{In}_2\text{O}_5$ in this study is in good agreement with that reported by Goodenough et al. [5].

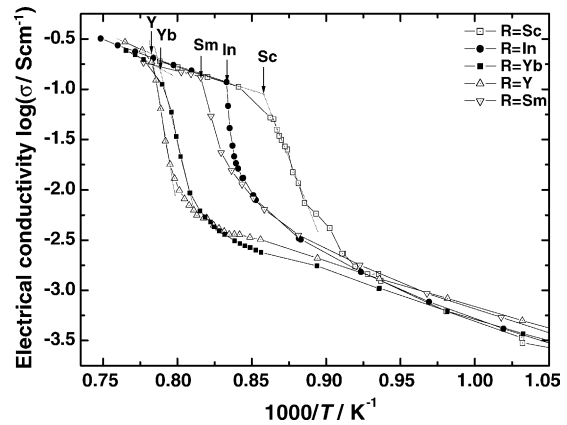


Fig. 5. Typical Arrhenius plots for $\text{Ba}_2(\text{In}_{0.9}\text{R}_{0.1})_2\text{O}_5$ ($\text{R} = \text{Sc}, \text{In}, \text{Yb}, \text{Y}, \text{Sm}$) system.

DTA curves of un-doped $\text{Ba}_2\text{In}_2\text{O}_5$ and $\text{Ba}_2(\text{In}_{0.9}\text{Sm}_{0.1})_2\text{O}_5$ as a function of temperature are shown in Fig. 6(a and b), where the T_t values determined by the electrical conductivity are also depicted. The T_t value of un-doped $\text{Ba}_2\text{In}_2\text{O}_5$ sample determined by the electrical conductivity measurement agrees well with the ending temperature of endothermic peak obtained by DTA method, but is slightly larger than the peak temperature. On the other hand, the T_t of the substituted $\text{Ba}_2(\text{In}_{0.9}\text{Sm}_{0.1})_2\text{O}_5$ is between the peak and ending temperatures measured by DTA method.

The order–disorder transition temperatures, T_t of $\text{Ba}_2(\text{In}_{1-x}\text{R}_x)_2\text{O}_5$ due to oxygen vacancies are plotted as a function of ionic radius of rare earth substituent in Fig. 7. The T_t of both compositions, $x = 0.05$ and 0.1 , increase with increasing ionic radius up to Y^{3+} ion, but decrease with further increasing the ionic radius. The order–disorder transition consists of two processes; the first process is due to the exchange of oxygen ions O(3) in the tetrahedral layers with un-occupied site O(3) in tetrahedral layer at around 1200 K, and the second process is due to the exchange of oxygen ions O(1) and O(2) with un-occupied site O(3) at around 1350 K [8,9]. We

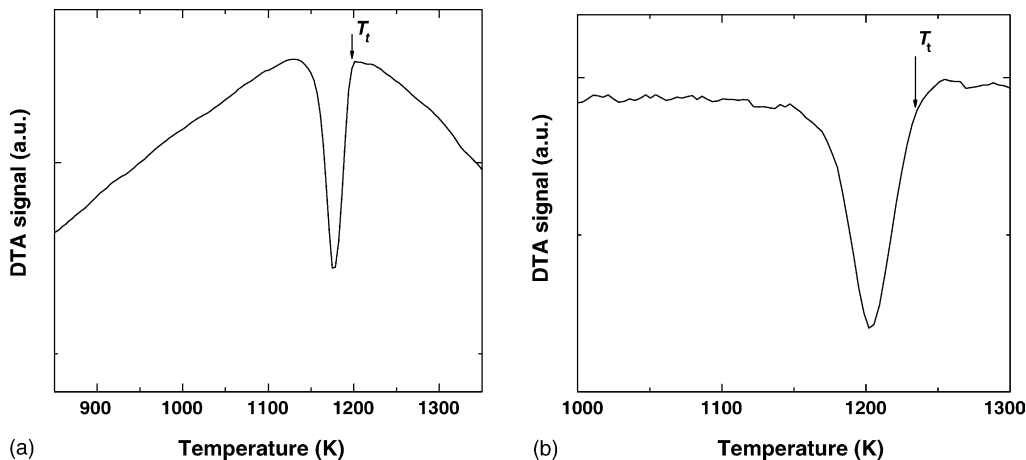


Fig. 6. DTA curves of: (a) un-doped $\text{Ba}_2\text{In}_2\text{O}_5$ and (b) $\text{Ba}_2(\text{In}_{0.9}\text{Sm}_{0.1})_2\text{O}_5$. The order–disorder transition temperature, T_t determined by the electrical conductivity measurement is shown by the arrow.

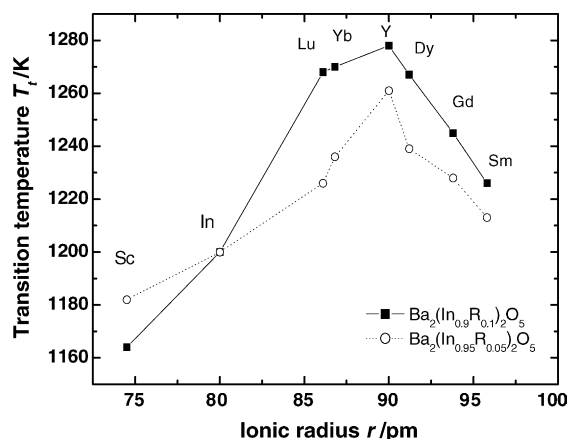


Fig. 7. Order–disorder transition temperature vs. ionic radius of substituents.

focus on the first process, because the measuring temperature range in this study is below 1323 K.

Let us discuss about the order–disorder transition from the viewpoint of the preferred site of substituents. In the mother compound, $\text{Ba}_2\text{In}_2\text{O}_5$, there is a cooperative tilt of tetrahedral InO_4 and octahedral InO_6 [9], which results from un-occupied sites O(3) in Fig. 1. The indium ion In(2) stays in the inside of tetrahedral InO_4 , but does not stay at the center of the square, which was formed by four sites O(3) 8(i) in tetrahedral layers (two occupied sites of oxygen ions O(3) and two un-occupied sites) as seen in Fig. 1. The shift of indium ions In(2) from the center of the square make higher potential energy of un-occupied sites than occupied sites O(3) [8].

The substitution with the smaller ionic radius like Ga^{3+} ion than In^{3+} ion favors settling in the tetrahedral site InO_4 [14]. In this viewpoint, we assume that the smaller substituting ions, such as Sc^{3+} will have higher probability of substitution for the indium ions In(2) in tetrahedral InO_4 than for the indium ions In(1) in octahedral InO_6 . The distance between substituents and oxygen ions O(3) will be decreased by the substitution of Sc^{3+} , and the substituents shift to the center of the square. This shift can decrease the potential energy of un-occupied sites to potential energy which is approximately equivalent to potential energy of occupied sites, and thus, the hopping probability of oxygen ion O(3) from occupied sites to un-occupied sites in tetrahedral layer will be higher. It means that the oxygen ion requires a smaller thermal energy in order to move to un-occupied sites. These easily hopping oxygen ions may stimulate the decrease of the order–disorder transition temperature. On the other hand, for the substitution of Lu^{3+} , Yb^{3+} , Y^{3+} , Dy^{3+} , Gd^{3+} and Sm^{3+} ions with larger ionic radius than In^{3+} ion, these ions will favor substituting for the indium ions In(1) in octahedral InO_6 [13]. The probability of locating substituents in octahedral site InO_6 is increasingly higher than in tetrahedral site InO_4 . This substitution will increase the distance between indium ions R(1) and oxygen ions O(2) and thus, forces the oxygen ions O(2) to get closer to tetrahedral layers. The distance between O(2) and un-occupied site O(3), can be decreased

by substitution with larger ionic radius than In^{3+} and make higher probability of exchange between O(2) oxygen sites and un-occupied sites O(3). This may cause lowering the order–disorder transition temperature. A maximum transition temperature at Y^{3+} -substituted sample may be related to the change in the slope of lattice parameter against ionic radius. In order to solve this problem, thermodynamic data of transition enthalpy and entropy for the substituted samples are needed and now are in progress in our laboratory.

4. Conclusions

The lattice volumes of $\text{Ba}_2(\text{In}_{1-x}\text{R}_x)_2\text{O}_5$ substituted for In site by rare earth elements showed a linear relationship between the lattice volume and substituted content up to $x = 0.1$ and increased with increasing ionic radius of the substituents. The change in the slope of the lattice volume against the ionic radius of substituent was found around the ionic radius of Y^{3+} or Dy^{3+} ions.

The order–disorder transition due to oxygen vacancies was observed for all prepared samples in DTA and electrical conductivity measurements. The order–disorder transition temperatures were increased (or decreased) by the substitution with higher (or lower) ionic radius than In^{3+} ion. This tendency may be explained by the preferred site of substituent to two In sites of octahedral InO_6 and tetrahedral InO_4 sites.

References

- [1] A.F. Sammels, R.L. Cook, J.H. White, J.J. Osborne, R.C. MacDuff, *Solid State Ionics* 52 (1992) 111–123.
- [2] K.R. Kendall, C. Navas, J.K. Thomas, H.C. Loye, *Solid State Ionics* 82 (1995) 215–223.
- [3] H. Hayashi, H. Inaba, M. Matsuyama, N.G. Lan, M. Dokiya, H. Tagawa, *Solid State Ionics* 122 (1999) 1–15.
- [4] J.B. Goodenough, *Annu. Rev. Mater. Res.* 33 (2003) 91–128.
- [5] J.B. Goodenough, J.E. Ruiz-Diaz, Y.S. Zhen, *Solid State Ionics* 44 (1990) 21–31.
- [6] J.B. Goodenough, A. Manthiram, P. Paranthaman, Y.S. Zhen, *Solid State Ionics* 52 (1992) 105–109.
- [7] T.R.S. Prasanna, A. Navrotsky, *J. Mater. Res.* 8 (1993) 1484–1486.
- [8] S.B. Adler, J.A. Reimer, J. Baltisberger, U. Werner, *J. Am. Chem. Soc.* 116 (1994) 675–681.
- [9] S.A. Speakman, J.W. Richardson, B.J. Mitchell, S.T. Mixture, *Solid State Ionics* 149 (2002) 247–259.
- [10] C.A.J. Fisher, B. Derby, R.J. Brook, *Br. Ceram. Proc.* 56 (1996) 25–31.
- [11] H. Yamamura, Y. Yamada, T. Mori, T. Atake, *Solid State Ionics* 108 (1998) 377–381.
- [12] V. Jayaraman, A. Magrez, M. Caldes, O. Joubert, M. Ganne, Y. Piffard, L. Brohan, *Solid State Ionics* 170 (2004) 17–24.
- [13] Y. Uchimoto, M. Kuniyama, T. Yao, *Jpn. J. Appl. Phys.* 38-1 (1999) 111–114.
- [14] T. Yao, Y. Uchimoto, M. Kinuhata, T. Inagaki, H. Yoshida, *Solid State Ionics* 132 (2000) 189–198.
- [15] Y. Liu, R.L. Withers, J.F. Gerald, *J. Solid State Chem.* 170 (2003) 247–254.